Polymer 50 (2009) 1596–1601

Contents lists available at ScienceDirect

Polymer

journal homepage: www.elsevier.com/locate/polymer

A novel type of shape memory polymer blend and the shape memory mechanism

Heng Zhang, Haitao Wang, Wei Zhong*, Qiangguo Du*

Key Laboratory of Molecular Engineering of Polymers of Ministry of Education, Department of Macromolecular Science, Fudan University, Shanghai 200433, China

ARTICLE INFO

Article history:
Received 14 June 2008
Received in revised form
12 October 2008
Accepted 9 January 2009
Available online 14 January 2009

Keywords:
Shape memory polymer
Polymer blend
Shape memory mechanism

ABSTRACT

A novel styrene–butadiene–styrene tri-block copolymer (SBS) and poly(ε-caprolactone) (PCL) blend were introduced for its shape memory properties. Compared to the reported shape memory polymers (SMPs), this novel elastomer and switch polymer blend not only simplified the fabrication process but also offer a controllable approach for the study of mechanisms and the optimization of shape memory performances. Microstructures of this blend were characterized by differential scanning calorimetry (DSC), AFM microscope observation and tensile test. DSC results demonstrated the immiscibility between SBS and PCL. AFM images and stress–strain plot further confirmed the two-phase morphology within the blend. It was found that the SBS and PCL continuous phases contributed to the shape recovery and shape fixing performances, respectively. A detailed shape memory mechanism for this type of SMP system was then concluded and an optimized SMP system with both good recovery and fixing performances was designed from this mechanism.

1. Introduction

Thermo-responsive shape memory polymers (SMPs) are those which have the capability of changing their shapes from a temporary shape to a permanent shape upon application of an external thermal stimulus [1,2]. It attracted great attention of scientists and engineers due to the novel capacity to be manipulated into one desired shape and then recover to another desired shape when temperature varies from below to above the transition temperature. It provides great potential for applications in sensors, actuators, packaging, medical materials, etc [3–5].

The recent study on SMPs was abundant. To our knowledge, recent SMPs can be classified into two main categories. One is polymer networks, including covalently cross-linked and physically cross-linked amorphous or crystalline copolymers [6–9]. The other is polymer blend [3,10].

For SMPs based on polymer networks, their shape memory mechanisms have already been ascribed to the cooperation of the hard and soft segments of the copolymers. Phase separation is required in this mechanism. Hard segments should be the droplet phase and act as the cross-links. Soft segments should be the matrix phase and act as the switch [1,2]. The clear mechanism offers a simple way to design the polymer networks to achieve good shape memory properties. But likewise, the synthesis and the characterization of the designed networks are both complicated and inconvenient.

Polymer blending offers a much simpler way to fabricate SMPs. The type of blends described in literatures usually consists of an amorphous polymer and a crystalline polymer and the two components should be melt-miscible, like PVDF/PMMA [3], PVDF/PVAc [3] and PLA/PVAc [3,10], etc. But due to the few reports in literatures, the shape memory mechanism and the relationship between the phase morphology and shape memory properties were still not obvious for SMPs based on polymer blends.

To address these questions, we report a novel type of shape memory polymer blends, which is simple to fabricate and easy to design to achieve good shape memory properties. This blend consists of two immiscible components, one is an elastomer and the other is a switch polymer. The elastomer can be any rubber or thermoplastic elastomer and the switch polymer can be any amorphous or crystalline polymer. Due to their immiscibility, samples with various controlled phase morphology can be prepared for the study of shape memory mechanism and the optimization of shape memory performance can be achieved with optimized phase morphology.

To substantiate this novel type of blend, we selected styrene–butadiene–styrene tri-block copolymer (SBS) as the elastomer and poly(ε-caprolactone) (PCL) as the switch polymer. The miscibility, thermal and mechanical properties, and the relationship between phase morphology and shape memory properties were studied in

* Corresponding authors. Tel.: +86 21 6564 3891; fax: +86 21 6564 0293.
E-mail addresses: qgdu@fudan.edu.cn (W. Zhong), weizhong@fudan.edu.cn (Q. Du).

0032-3861/$ – see front matter © 2009 Elsevier Ltd. All rights reserved.
doi:10.1016/j.polymer.2009.01.011

Table 1
Labels of the samples.

Labels	PCL0	PCL10	PCL20	PCL30	PCL50	PCL70	PCL80	PCL90	PCL100
PCL content (wt%)	0	10	20	30	50	70	80	90	100
SBS content (wt%)	100	90	80	70	50	30	20	10	0

this paper. Finally, a mechanism and an optimization design for this type of SMP blend were proposed and testified.

2. Experimental

2.1. Materials

Styrene–butadiene–styrene tri-block copolymer (SBS, YH-791) was purchased from Balin Petrolem Chemical Corporation, Sinopec Group, China. The weight proportion of polystyrene/polybutadiene is 30/70. $M_n = 1.46 \times 10^5$, $M_w/M_n = 1.09$. Poly(ε-caprolactone) (PCL, Capa 680, Batch 108) was purchased from Solvay Interox Ltd. $M_n = 1.40 \times 10^5$, $M_w/M_n = 1.50$. These materials were used without further purification. The molecular characteristics of the polymers were determined by gel permeation chromatography (GPC, Agilent1100).

2.2. Preparation of SBS and PCL blend samples and phase morphology observation

SBS and PCL were blended in a Banbury mixer (PLE 651, Brabender, Germany) at 180 °C, 60 min^{-1} for 10 min. The PCL contents varied from 0 wt% to 100 wt%. The details were listed in Table 1. After blending, the samples were compressed into plates in a hot press at 180 °C with the pressure of 5 kg N m^{-2}.

And then the samples were fractured in liquid nitrogen and their cross-sections were observed by an atomic force microscope (AFM, SPM/STM-9500J3, Shimadzu, Japan). Phase modulus of AFM was applied to reveal the phase morphology.

2.3. Determination of glass transition and melting temperatures

The glass transition and melting temperatures (T_g and T_m) of the samples were determined with differential scanning calorimetry (DSC, Pyris 1, Perkin Elmer, USA). To achieve good sensitivity, two steps were performed. First the samples were heated from 0 °C to 120 °C at a constant rate of 10 °C min^{-1}, and T_ms were determined by this step. Second, quench the samples to −100 °C after holding in 120 °C for 3 min. And then, T_gs were determined when the samples were heated from −100 °C to 120 °C at a constant rate of 10 °C min^{-1}.

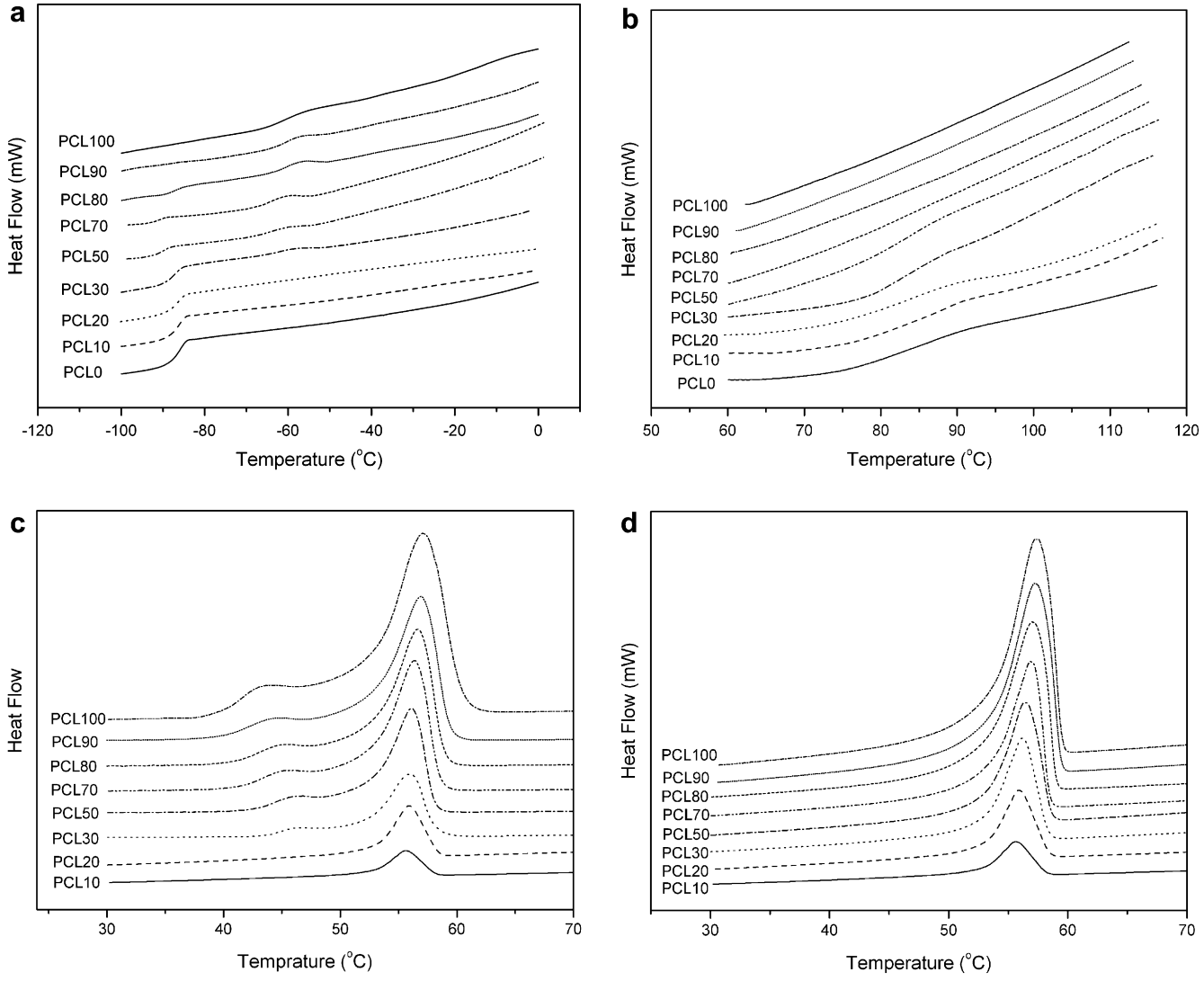

Fig. 1. The DSC plots of each sample. (a) T_gs of PCL and PB on the second run. (b) T_g of PS on the second run. (c) T_m of PCL on the first run. (d) T_m of PCL on the second run.

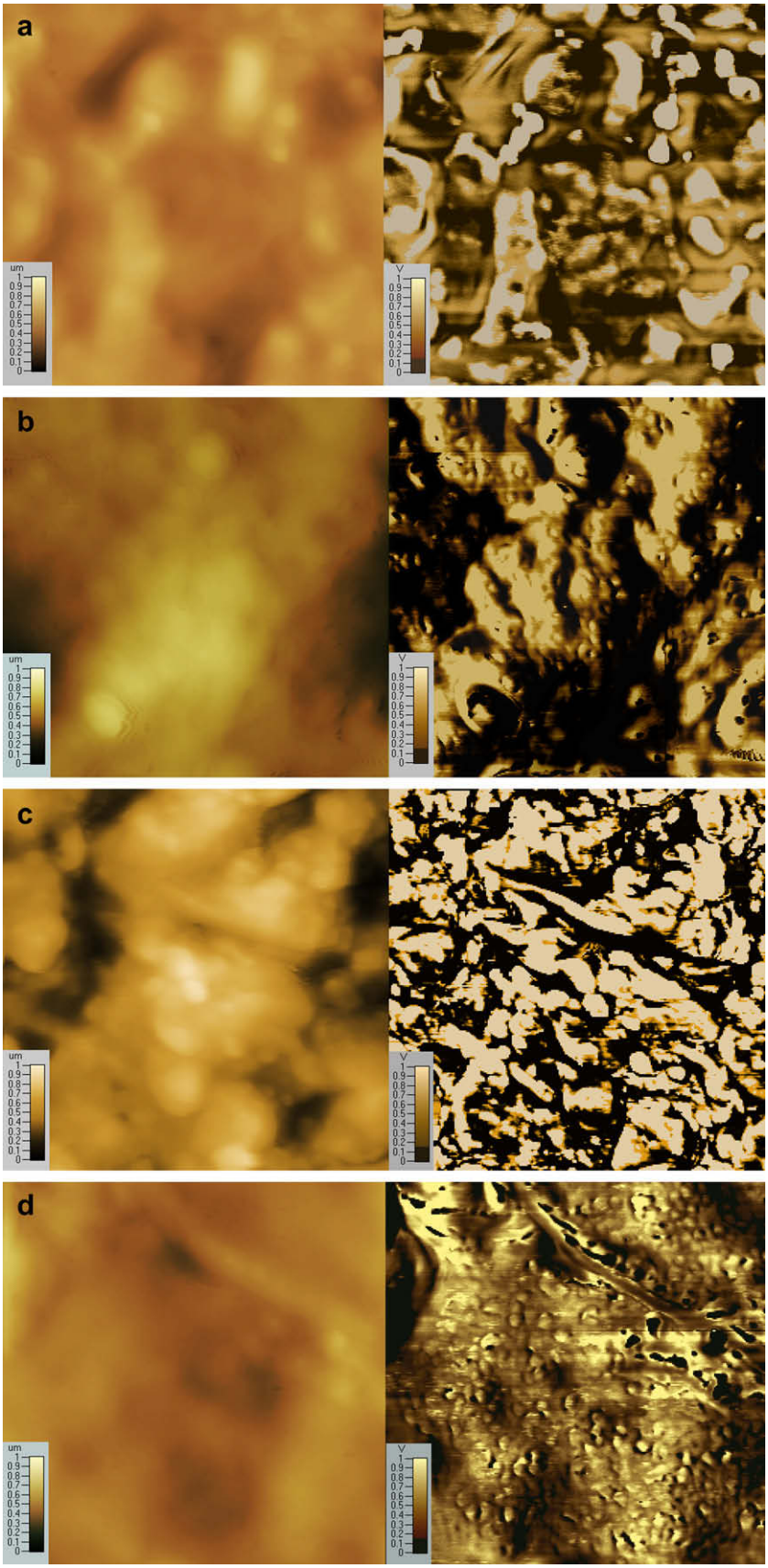

Fig. 2. The AFM images of the cross-sections of typical SBS/PCL blend samples. (a) PCL20, (b) PCL30, (c) PCL70, (d) PCL90. The left images were for height and the right images were for phase. The ranges of each image were all 5 μm × 5 μm.

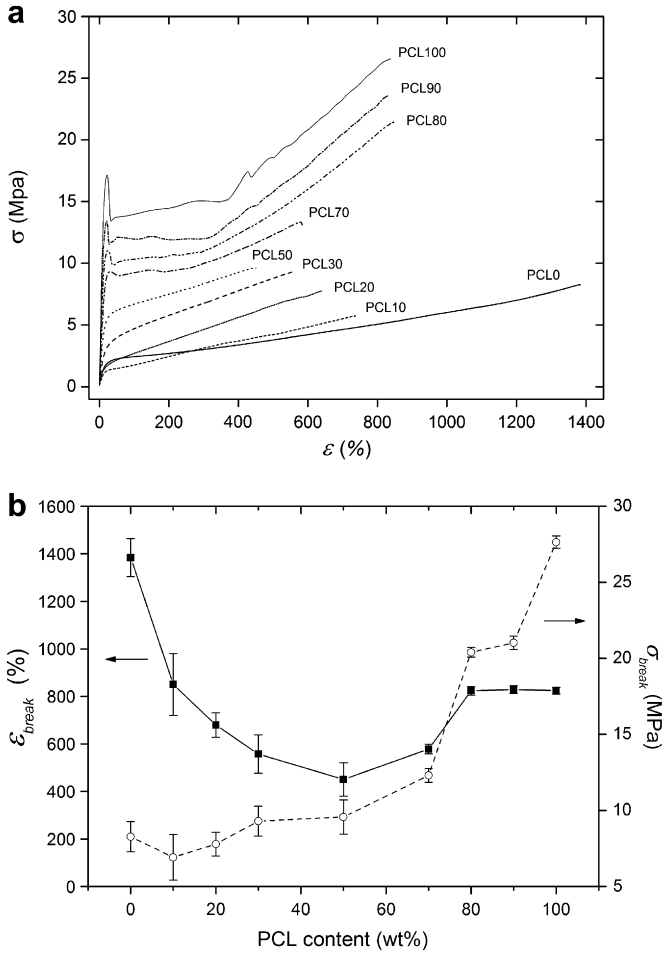

Fig. 3. (a) Stress–strain plot of each sample. (b) The dependence of elongation at break (ε_{break}), stress at break (σ_{break}) and PCL content.

2.4. Tensile test and shape memory test

Tensile tests at room temperature were carried out on a tensile test instrument (SANS PowerTest v3.0, Shenzhen SANS Material Test Instrument Co. Ltd., China) according to ASTM D412. The strain rate was 10 mm min^{-1}. Strain–stress plots were recorded during the experiment.

Shape memory test was carried out according to the following steps. (1) Heating up the sample to 80 °C and holding for 5 min. (2) Extending the sample to the strain of 100% (ε_m). (3) Cooling down the sample to 20 °C in the extended state and holding for 5 min. (4) Unloading the sample to zero stress and then recording the strain (ε_u). (5) Heating up the sample to 80 °C again and holding for 5 min and then recording the strain (ε_p). Shape recovery ratio (R_r) and shape fixing ratio (R_f) were calculated by the following equations, respectively. Five samples of each PCL content were measured to achieve the average R_r and R_f.

$$R_r = \frac{\varepsilon_m - \varepsilon_p}{\varepsilon_m} \quad (1)$$

$$R_f = \frac{\varepsilon_u}{\varepsilon_m} \quad (2)$$

3. Results and discussion

3.1. Miscibility of SBS and PCL blend

The thermal properties of SBS and PCL blends were determined by differential scanning calorimetry (DSC). Fig. 1a–d showed the DSC plots of each sample labeled from PCL0 to PCL100.

Glass transition temperatures of the SBS/PCL blend systems with different compositions were obtained from Fig. 1 for the discussion of the miscibility between components. The presence of three T_gs of PCL, PB and PS in sample PCL30 and PCL50 indicated the immiscibility of the three components, which was consistency with the literatures [11,12]. For sample PCL10 and PCL20, the T_gs of PCL could not be unambiguously determined. But the almost unchanged T_gs of PB's and PS's indicated their immiscibility with PCL. And the invisible glass transitions of PCL were then probably due to the low PCL contents. The same conclusion can be drawn in PCL70 and PCL80, which showed the almost invariable T_gs of PB and PCL.

From the above discussions, the immiscibility between PCL, PB and PS segments in SBS/PCL blends could be confirmed. But in consideration of the covalent-bond-links between PB and PS chains, SBS was taken into account as one phase compared with the other PCL phase in our paper. And thus, the immiscibility of the three components would then induce the morphology of phase separation between SBS and PCL in their blends.

For the discussion of melting temperatures (T_m), from Fig. 1c, there were shoulders in the melting peaks of several blend systems (PCL30–PCL100), these shoulders might be caused by the thermal history because they disappeared in the second run (Fig. 1d). The T_ms of PCL could be taken as the shape memory transition temperatures (T_{trans}) of the blends. The T_{trans} didn't change too much with the PCL content, which may due to the immiscibility between SBS and PCL.

3.2. Microstructures of SBS/PCL blends

Inasmuch as the blend consists of a hard phase (PCL) and a soft phase (SBS), atomic force microscope was applied to reveal the phase morphology. Fig. 2 showed the AFM images of each sample. The left images were for height and the right images were for phase, where the bright region was PCL phase and the dark region was SBS phase. The ranges of each image were all 5 μm × 5 μm.

Because of the intrinsic immiscibility between SBS and PCL components, there are always phase separations in their blends. With the increasing content of PCL, PCL phase would transform from a droplet-like dispersion phase to a continuous phase, and then to the matrix. Fig. 2 clarified the transformation. Below content of 20 wt% (Fig. 2a), PCL was the droplet phase and SBS was

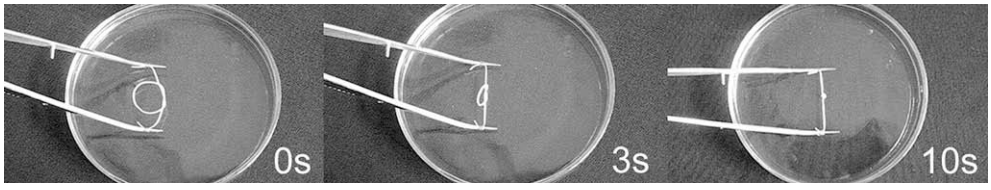

Fig. 4. An example for the recovery process of shape memory effect when the PCL50 sample was placed in water of 70 °C.

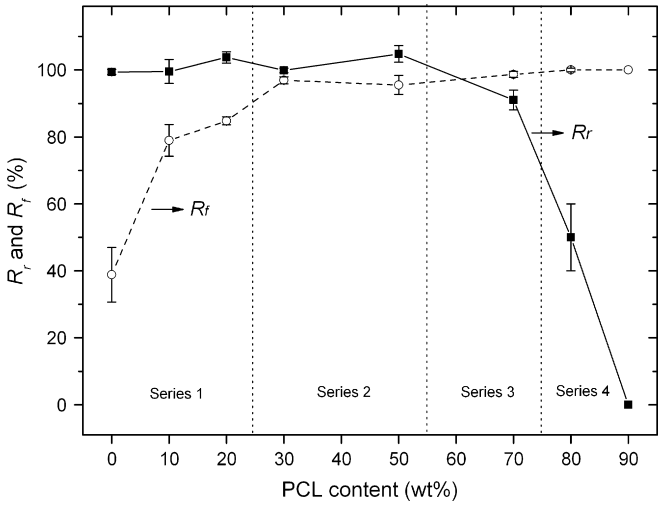

Fig. 5. Shape recovery ratio (R_r) and shape fixing ratio (R_f) of each sample.

the matrix. From content of 30 wt% (Fig. 2b), PCL phase became more and more continuous. After content of 70 wt% (Fig. 2c), PCL began to form the matrix and SBS phase became discrete. When PCL content reached 90 wt% (Fig. 2d), SBS component completely changed to droplet-like dispersion phase.

From the above discussion, we knew the samples of bi-continuous morphology were from PCL30 to PCL70. They were obtained under our preparation condition described in Part 2.2. These phase morphology analysis helped to understand the mechanical properties and shape memory properties of the SBS/PCL blends.

3.3. Mechanical properties of SBS and PCL blend

Each sample blends was characterized by tensile tests at room temperature. The stress–strain (σ–ε) plots were illustrated in Fig. 3a. The dependence of elongation at break (ε_{break}), stress at break (σ_{break}) on PCL content was shown in Fig. 3b.

In view of the typical elastomeric characteristic of SBS and the typical thermoplastic characteristic of PCL, respectively, the presence of SBS matrix should have no yield point in the σ–ε plot while the presence of PCL matrix should result in yield point. According to this, from Fig. 3a, when PCL contents were below 50 wt%, no yield points were observed, which was due to the SBS matrix in the blends. While the PCL contents were above 50 wt%, yield points were observed because PCL became the matrix phase in these samples. But for PCL70 sample, the yield point was not distinct and not any notable neck was observed while stretching. It may due to the existence of SBS continuous phase in this blend with bi-continuous phases (Fig. 2c).

Neat SBS and PCL showed big difference in ε_{break} and σ_{break} as illustrated in Fig. 3b. The addition of PCL into SBS reduced the ε_{break} from almost 1400% to around 500% at most. And the σ_{break} increased with the PCL content, which came from the relatively high σ_{break} value of the neat PCL.

During the tensile tests, we didn't observe any notable delamination of the samples. In view of the immiscibility between SBS and PCL, the adhesion between the two phases was supposed to be low. But from the AFM images, the phase sizes were only in the range of several micrometers. The topology of the micro-phase-separation morphology may help to prevent the macro-scale delamination.

Table 2
Details of regions in Fig. 5.

Region	Samples	Typical phase morphology image(s)	Shape recovery performance	Shape fixing performance
1	PCL0, PCL10, PCL20	Fig. 2a	Good	Bad
2	PCL30, PCL50	Fig. 2b	Good	Good
3	PCL70	Fig. 2c	Good	Good
4	PCL80, PCL90	Fig. 2d	Bad	Good

3.4. Shape memory properties of SBS and PCL blend

Fig. 4 showed an example for the recovery process of shape memory effect when the PCL50 sample was placed in water of 70 °C. The sample automatically knotted within 10 s, which was due to the transition from temporary shape to permanent shape. The simple fabrication and fast recovery process could find the application in thermo-sensitive sutures for example.

The detailed shape memory properties were represented by shape recovery ratio (R_r) and shape fixing ratio (R_f) according to the literatures [1,6]. R_r and R_f of each SBS/PCL blend sample were calculated and illustrated in Fig. 5.

From Fig. 5, the R_r dropped from about 100% to zero after PCL content of 50 wt% and R_f shifted from about 40% to 100% after PCL content of 30 wt%. It indicated that the networks of SBS contributed to shape recovery performance (R_r) and the crystallization of PCL contributed to shape fixing performance (R_f). Fig. 5 was divided into four regions for further discussion. The details of each region were presented and analyzed in Table 2.

Region 1 showed good shape recovery performance but bad shape fixing performance. The shape recovery ratios (R_r) of these three samples were all near 100%, which was due to the highly elastic SBS matrix phase. And for shape fixing ratios (R_f), PCL10 and PCL20 showed much better shape fixing performance than the neat SBS (PCL0), due to the crystallization of the fixing component of PCL. But with such low content, PCL could only form the droplet phase (Fig. 2a). Its crystallization could not strongly resist shape recovery, and therefore the shape fixing performance was not as good as the other regions.

Region 2 showed both good shape recovery and good shape fixing performances. PCL30 and PCL50 both showed R_r of near 100%, which was also due to the SBS matrix. While for R_f, there was a shift from about 80% to above 95% from region 1 to region 2. As we discussed above (Fig. 2b), PCL continuous phase began to form in PCL30. And hence, the crystallization of continuous PCL phases in the SBS matrix would set an effective resistance to the shape recovery. Therefore, the shift of R_f originated in the PCL continuous phase in region 2, which contributed to the good shape fixing performance.

Region 3 showed similar shape memory property like region 2 but with different phase morphology. PCL began transferring to the matrix, which retained the good shape fixing performance. During this transformation, there were still some SBS continuous phase existed (Fig. 2c), which could account for the fact that the R_r was only slightly reduced to about 90%.

Region 4 showed bad shape recovery performance but good shape fixing performance. The PCL matrix resulted in good shape fixing performance and the dispersed SBS droplet phase (Fig. 2d) resulted in the shift of R_r from about 90% to zero.

3.5. Mechanism of shape memory properties of elastomer/switch polymer blend and the optimized design of shape memory performances

According to the above investigation, the shape memory mechanism of elastomer/switch polymer blends can be concluded

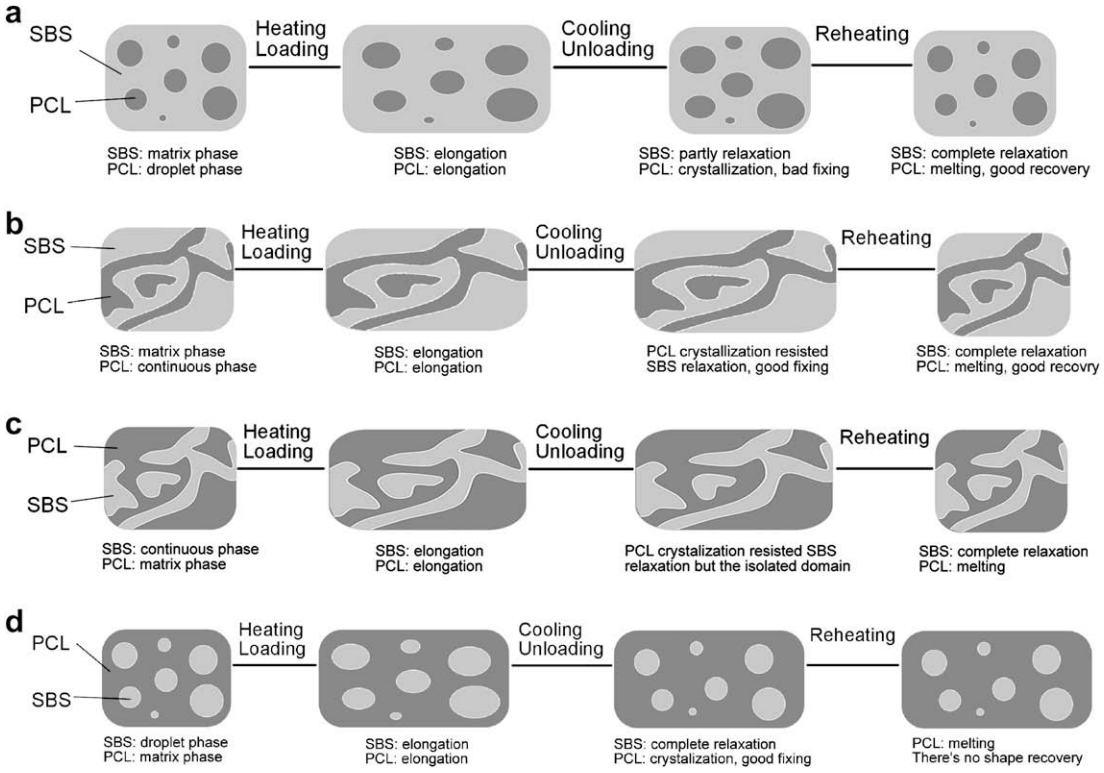

Fig. 6. Schematic figures of the shape memory mechanism of elastomer/switch polymer blends concluded from SBS/PCL blend.

from the SBS/PCL blend system. This type of SMPs requires two immiscible components. One is the elastomer, which can be any rubberlike or thermoplastic elastomers. The other is the switch polymer, which can be any crystalline polymers. These two phases contribute to shape recovery and fixing performances respectively. In detail, the shape memory mechanism can be classified into four series with different phase morphologies illustrated in Fig. 6. Table 3 showed the details for each series.

Due to the immiscibility, phase separation always takes place in this blend system. Through careful design of the immiscible phase morphology, an ideal SMP system with both good stability and performances can be achieved. From Table 3, the optimized design will be series 2 with elastomer being major continuous phase and switch polymer being minor continuous phase. In this optimized design, the elastic matrix provides the good stretching and recovery performance while the continuous switch polymer phase affords the good fixing and unfixing performance while hardly reduces the recovery performance.

4. Conclusion

SBS and PCL blend were introduced as the example of a new type of elastomer/switch polymer immiscible blend SMP system. DSC results demonstrated the immiscibility between SBS and PCL phases and the shape memory transition temperatures were in the range of 56–57 °C. AFM images and stress–strain plots both clarified the phase-separation morphology. Under our experiment condition, below content of 20%, PCL was droplet phase. From content of 30%, PCL began to form continues phase. After content of 70%, PCL began transferring to matrix.

From the shape memory investigation results, a general shape memory mechanism for this type of polymer blend SMP was proposed that the two immiscible components of the blend separates contributed respectively to shape memory performances. The elastomer provided the stretching and recovery performances and the switch polymer provided the fixing and unfixing performances. An optimized design of phase morphology is then concluded, which contains the elastomer major continuous phase and switch polymer minor continuous phase.

Table 3
Details for each series of mechanism.

Series	Figures	Phase morphology		Shape recovery performance	Shape fixing performance
		Elastomer	Switch polymer		
1	Fig. 6a	Matrix	Droplet	Good	Bad
2	Fig. 6b	Matrix	Continuous	Good	Good
3	Fig. 6c	Continuous	Matrix	Slightly reduced	Good
4	Fig. 6d	Droplet	Matrix	Bad	Good

References

[1] Lendlein A, Kelch S. Angew Chem 2002;41:2034–57.
[2] Behl M, Lendlein A. Mater Today 2007;10:20–8.
[3] Liu C, Qin H, Mather PT. J Mater Chem 2007;17:1543–58.
[4] Gunes IS, Cao F, Jana SC. Polymer 2008;49:2223–34.
[5] Yang B, Huang WM, Li C, Li L. Polymer 2006;47:1348–56.
[6] Lendlein A, Schmidt AM, Langer R. PNAS 2001;98:842–7.
[7] Rousseau IA, Mather PT. J Am Chem Soc 2003;125:15300–1.
[8] Liu C, Chun SB, Mather PT, Zheng L, Haley EH, Coughlin EB. Macromolecules 2002;35:9868–74.
[9] Lee BS, Chun BC, Chung YC, Sul KI, Cho JW. Macromolecules 2001;34:6431–7.
[10] Liu C, Mather PT. Proceedings of the annual technical conference – society of plastics engineers, 61st, vol. 2. Brookfield, CT, USA: Society of Plastics Engineers; 2003. 1962–6.
[11] Balsamo V, de Navarro CU, Gil G. Macromolecules 2003;36:4507–14.
[12] Balsamo V, Gil G, de Navarro CU, Hamley IW, von Gyldenfeldt F, Abetz V, et al. Macromolecules 2003;36:4515–25.